



UNITED NATIONS EDUCATIONAL, SCIENTIFIC AND CULTURAL ORGANIZATION
INTERNATIONAL ATOMIC ENERGY AGENCY
INTERNATIONAL CENTRE FOR THEORETICAL PHYSICS
I.C.T.P., P.O. BOX 586, 34100 TRIESTE, ITALY, CABLE: CENTRATOM TRIESTE



SMR.961 - 8

**WORKSHOP ON:
PROTEINS, MEMBRANES and their INTERACTIONS**

22 JULY - 2 AUGUST 1996

**"Mechanics and statistical mechanics
of fluid lipid-bilayer structures"**

**Michael WORTIS
Simon Fraser University
Department of Physics
British Columbia
V5A 1S6 Burnaby
CANADA**

These are preliminary lecture notes, intended only for distribution to participants.

Mechanics + Statistical Mechanics of Fluid-Phase Lipid-Bilayer Structures in Aqueous Solution

with Biological Applications!

Michael Wortis, Simon Fraser University, CANADA

At "Workshop on Proteins, Membranes, + Their Interactions"
Trieste, I.C.T.P., July 22-24, 1996

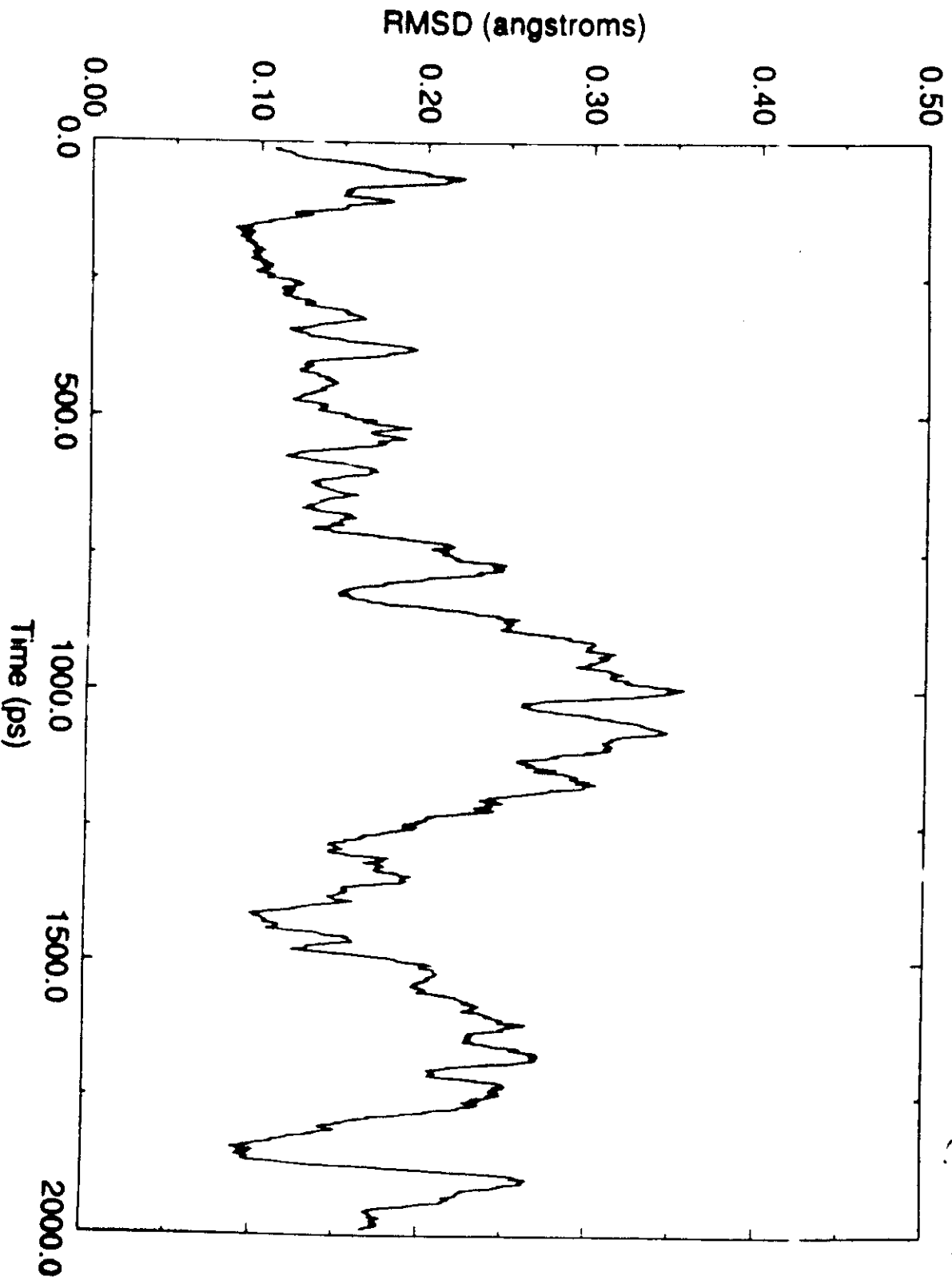
D. Beal (SFU)
E. Evans (UPC)
M. Bloom (UPC)
R.N.P. Evans (UPC)

B. Ferrada
M. Rao
U. Saeft
S. Langer
F. Tüchler

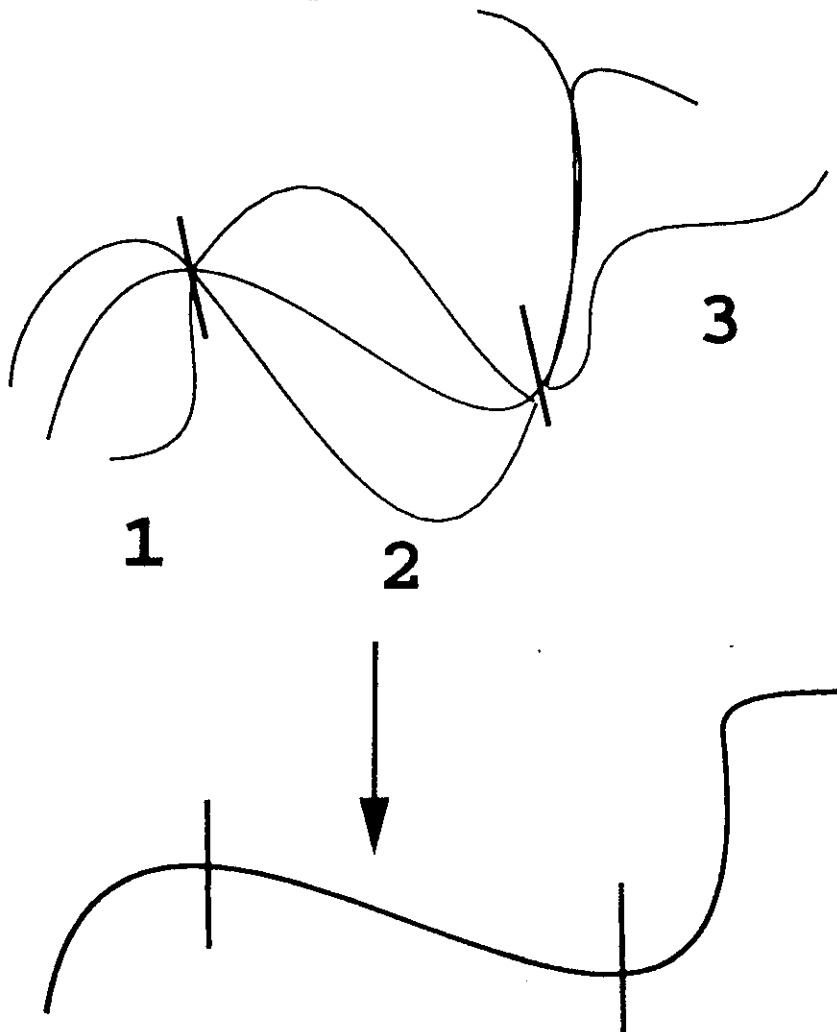
L. Mirre
H.-G. Döbereiner
M. Mirkovic (Miric)
+ Helfrich (many others)
Sackmann ...
Lipowsky

1. Introduction Phospholipid Chemistry
Membrane Structure
Biological Applications
2. Aggregation Phenomena Lyotropic Phases, etc. (Sellen)
Bilayer Phases, Phase Transitions
3. Mesoscopic Description of Bilayer Shape Mechanics Hamiltonian (Landau)
Persistence length
Bilayer Phases (revisited)
Fluid vs tethered Membranes (Gompper)
4. Vesicle Shapes + Shape Fluctuations Shapes
Phase Diagram
Stability
Shape Fluctuations
Bidding.
⇒ Dynamics (Serfert)

Fluctuations of optimized CHDLFc (3000 K)



**LES: Locally Enhanced
Sampling to smooth energy
surface and to obtain more
sampling**

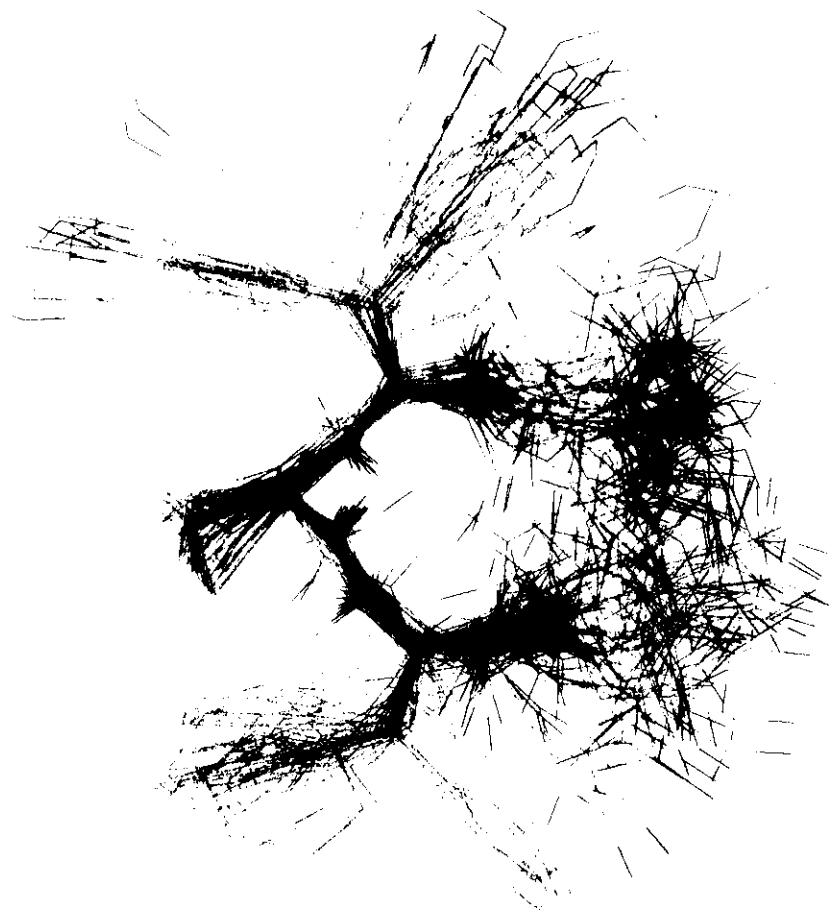


SYPFDV:

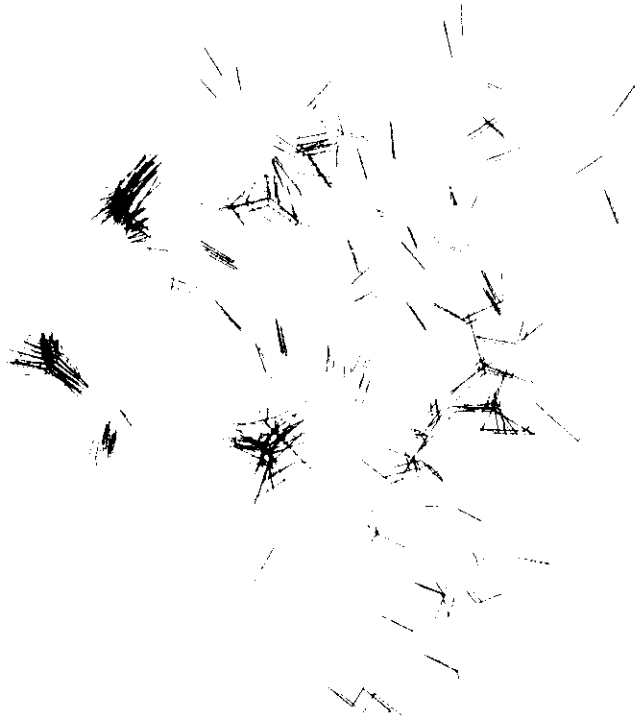
Electrostatic interactions between the C and N terminals induce the turn structure.

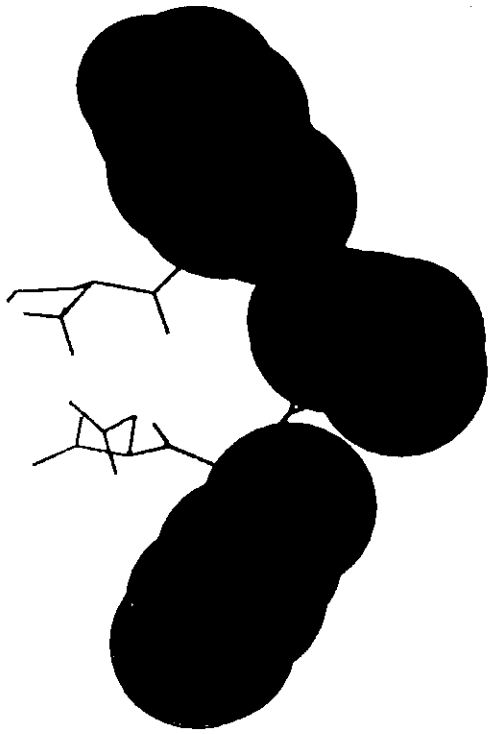
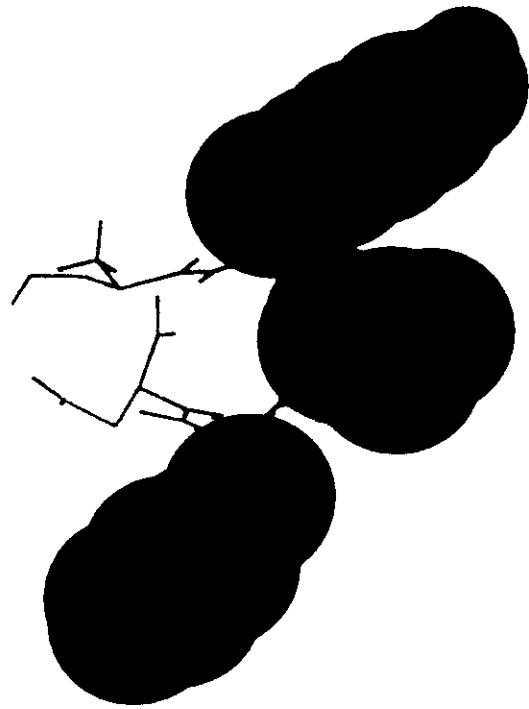
Hydrophobic interactions between the side chains come later. They are much weaker than the first and require considerably more gentle simulation conditions and the success rate is not that high as for the backbone

**Final Structures from Short Annealing Runs, superposed on NMR structure
using backbone atoms of TYR-PRO-PHE**



Final Structures from Long Anneling Runs, suppressed on NMR Resonance
using backbones of IYRHKCPHE

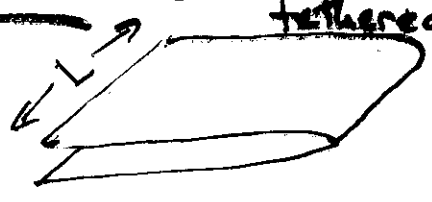




Apply Energy Entropy to Membrane (Fluid)

4. Can membrane remain aligned at $T > 0$? Yes (as it does for tethered)

$$E = \frac{\kappa_b}{2} \int dS (C_1 + C_2)^2$$



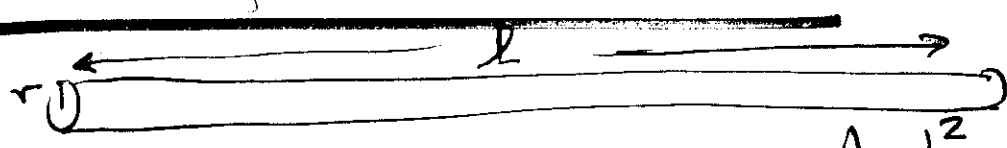
single crease of radius R

$$E = \frac{\kappa_b}{2} L R \left(\frac{1}{R}\right)^2 = \frac{\kappa_b}{2} \frac{L}{R}$$

$$g(E) \approx L^x \Rightarrow F = \frac{\kappa_b}{2} \frac{L}{R} - kT(\cdot) \ln L$$

c.f. $F=0$ at $T=0$

5. Can membrane lower its free energy by taking on linear shape?



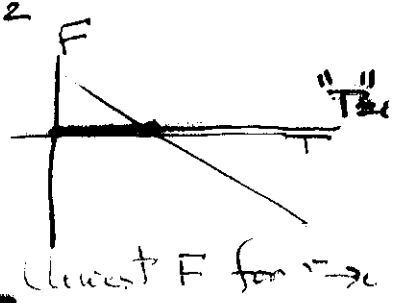
$$E = \frac{\kappa_b}{2} A \left(\frac{1}{r}\right)^2 \quad (\text{Energy cost})$$

$$A = L^2 = 2\pi r l$$

$$g(E) = q^{l/r} \quad (q = \# \text{ directions/bend})$$

$$S = k \ln g(E) = k \frac{l}{r} \ln q = \frac{kA}{2\pi} \frac{\ln q}{r^2}$$

$$F = \frac{1}{r^2} \left[\kappa_b - (\cdot) kT \ln q \right]$$



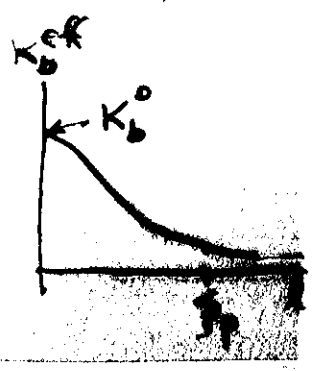
\Rightarrow (branched) polymer for $k_B T > \kappa_b$

Not quite right!

1. Renormalization of bending rigidity

$$\kappa_b^{eff}(l) = \kappa_b^0 \left[1 - \alpha \frac{kT}{\kappa_b^0} \ln(l/a) + \dots \right]$$

2. Microscopic length scale cuts off at ξ_p



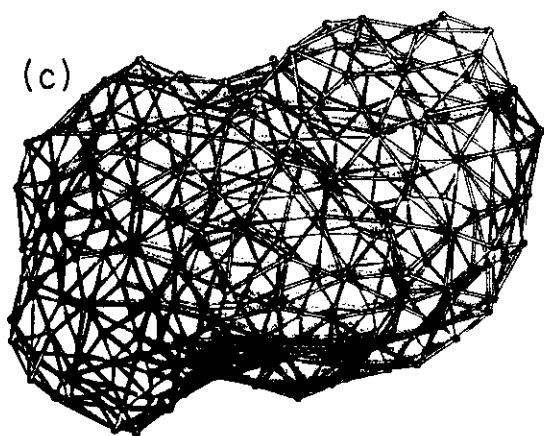
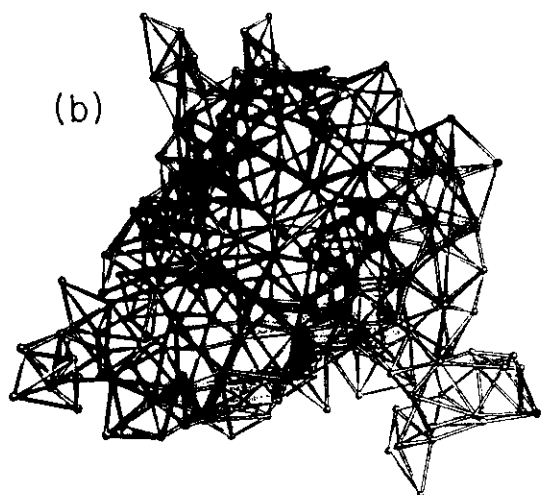
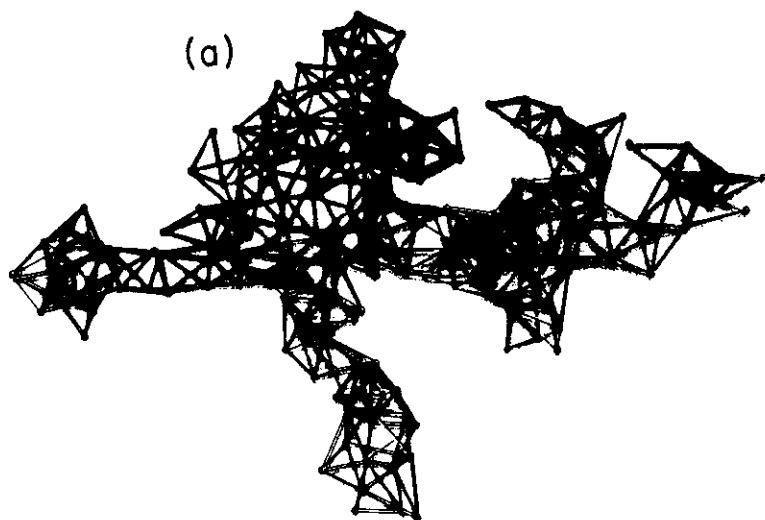


FIG. 2. Typical configurations of vesicles with $N = 247$ monomers. (a) $\lambda = 0.35$, $p = 0.125$ (branched polymer), (b) $\lambda = 0.35$, $p = 0.125$ (inflated), (c) $\lambda = 2.0$, $p = -0.05$ (prolate), (d) $\lambda = 2.4$, $p = -0.19$ (dumbbell), (e) $\lambda = 2.4$, $p = -0.35$ (branched polymer), (f) $\lambda = 3.0$, $p = -0.27$ (stomatocyte), (g) $\lambda = 3.8$, $p = -0.35$ (discocyte).

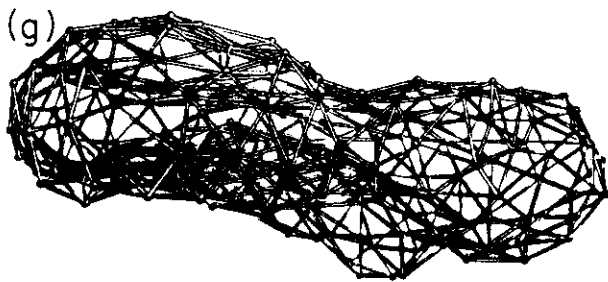
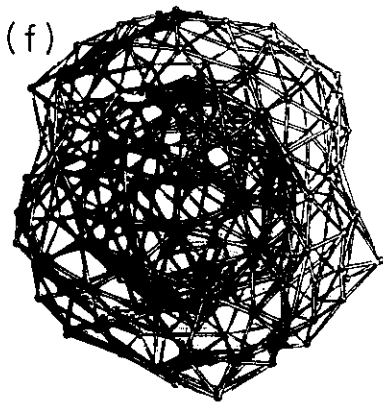
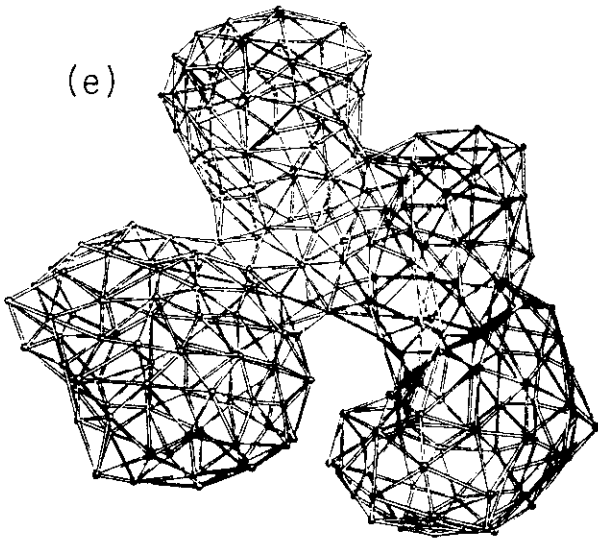
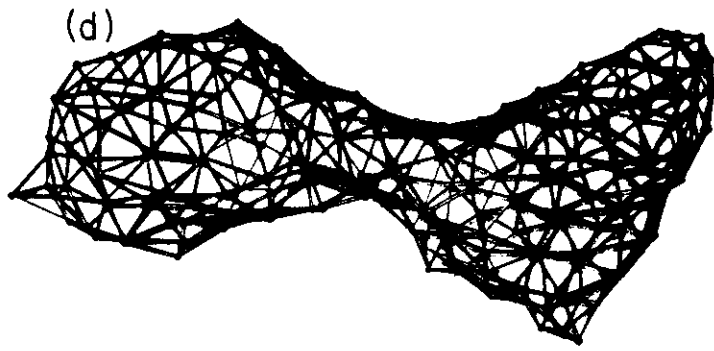


FIG. 2 (Continued).

What is the Hamiltonian $H[S]$ for describing closed micron-scale phospholipid vesicles?

39

$$H[S] = \gamma_0 \int dS + \left\{ \frac{1}{2} \kappa_b \int dS (c_1 + c_2 - c_0)^2 \right\} + \kappa_g \int dS c_1 c_2$$

Topology fixed

area fixed $A_0 \approx \frac{(N_1 + N_2) a_0(\tau)}{2}$

+ higher order in d/R $\frac{d}{R} \sim 10^{-3}$

+ λ edge edge large enough to close

Plus one additional term + subject to constraints

Overall stretching energy is large \rightarrow incompressibility $a(\vec{r}) \approx a_0(\tau)$

$$E_{str} = \frac{K}{2} \int dS \left(\frac{a(\vec{r}) - a_0}{a_0} \right)^2 \sim KR^2 \quad \text{vs } K(d^2)$$

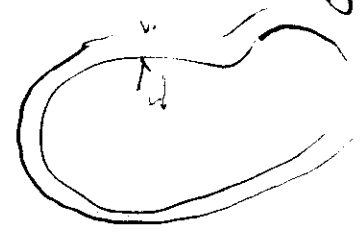
ie. $\frac{K(d^2)}{KR^2} \sim \frac{d}{R} \sim 10^{-3}$

BUT

It is not generally possible to have $a = a_0$ in both leaves of the bilayer simultaneously!

$$|\Delta A| \sim d \int dS (c_1 + c_2)$$

depends on shape



check for sphere:

$$\Delta A = d \cdot 4\pi R^2 \cdot \frac{2}{R} = 8\pi R d \quad \checkmark$$

(while) $\Delta A_0 = (N_1 - N_2) a_0$ fixed at closure

Comment: We might apply this as constraint on shape S .

But, better, simply allow individual monolayers to accommodate by making

$$a_{in}, a_{out} \geq a_0$$

COSTS ELASTIC ENERGY

Compare (estimate) elastic stretching cost w. bending:

$$\frac{K_b}{R^2} \approx 2 \cdot \frac{1}{2} \cdot \frac{K}{2} \cdot \left(\frac{\Delta T - \Delta T_c}{A_0} \right)^2 \sim \frac{K d^2}{R^2} \quad \text{same as bending energy density}$$

$\frac{1}{2} K_b (c_1 + c_2)^2$ $(d/R)^2$

$$H[S] = \frac{K_b}{2} \int dS (c_1 + c_2 - c_0)^2 + \frac{\bar{K}}{2} \frac{\pi}{A_0 d^2} (\Delta A[S] - \Delta A_0)^2$$

$\sim K \left(\frac{\Delta T - \Delta T_c}{A} \right)^2 \times A_0 \times \frac{d}{d^2}$

Where $a_{in} + a_{out}$ same over entire leaf (fluidity) but not quite equal to a_0 (or to each other)

\bar{K} called "nonlocal" bending modulus

$$\bar{K}/K_b \equiv \alpha \sim 1 \quad (\alpha_{sepc} \approx 1.4; \alpha_{DNPC} \approx 1.1)$$

(material parameter)

Expect laboratory shapes to be LOCAL minima of $H[S]$ subject to constraints of

- $V[S] = \text{constant}$ (importance of metastab since $\Delta E \sim K_b \gg k_B T$)
- $A[S] = \text{constant}$ (in practice determined by osmotic)
- $A_0 = \text{constant}$ (determined by $N_1 + N_2$)

Note V , A , and A_0 do change with T , since, e.g., $A_0 = \frac{1}{2}(N_1 + N_2) a_0(T)$
 $\Delta A_0 = (N_1 - N_2) a_0(T)$

Finding the local-minimum shapes:

(4)

1. Numerical: (Seifert et al.)

Triangulated surface S

Discrete representation of $H, V, A[S]$

Track energy to local minimum

Start again

conceptually simple
works for all kinds of shapes

But very time consuming
not very accurate. } unreliable for
singular shapes
near phase boundaries

2. Quasi-analytic:

Form variational functional to incorporate constraints

$$\Phi[S] = H[S] + \tau A[S] - p V[S]$$

Derive Euler equations: $\frac{\delta \Phi}{\delta S} = 0$ (Shape Equations)

highly nonlinear
multiple solns

Solve shape equations (numerical/analytic)

Find parameters τ, p

(check energy minima!)

only practical for axisymmetric shapes
(but, for high volumes, most important
shape branches are axisym!)

BUT, very accurate.

Results:

Shapes (shape classes)

"Phase Diagram" (lowest energy vs parameters)

stability (Regions where each shape class
is local minimum)

(Stability Boundaries)

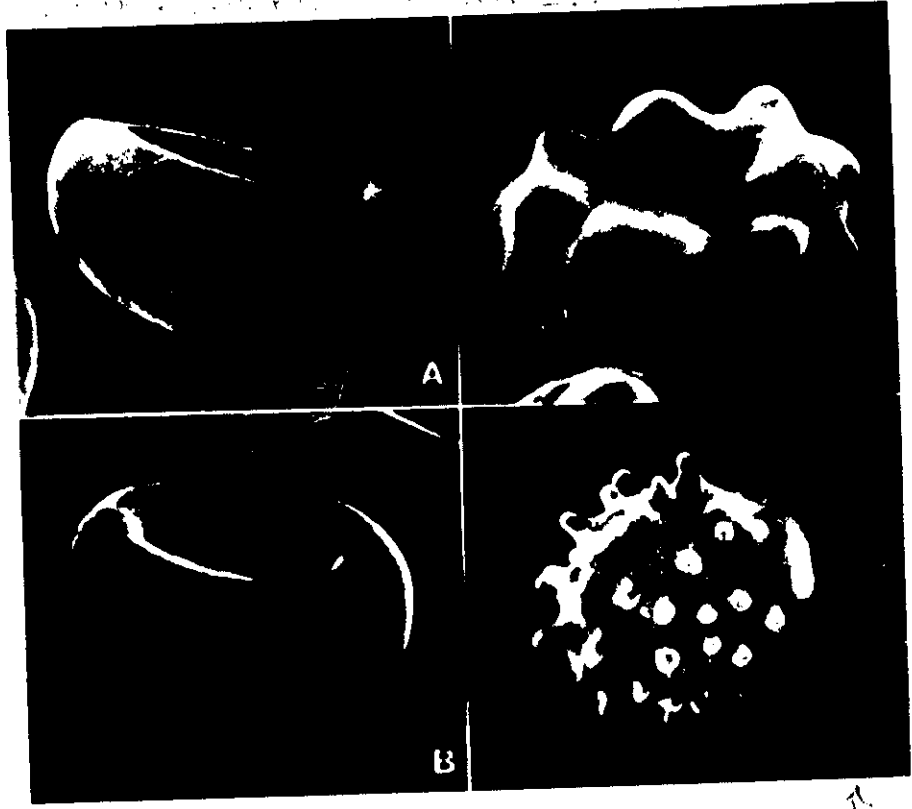


Fig. 1. Formes réversibles du globule rouge. A) Stomatocyte II; B) Stomatocyte III correspondant aux cellules 3 et 5 de la figure 3; C) Echinocyte II; D) Echinocyte III correspondant aux cellules 2 et 4 (gross. : $\times 8500$).

echinocyte.

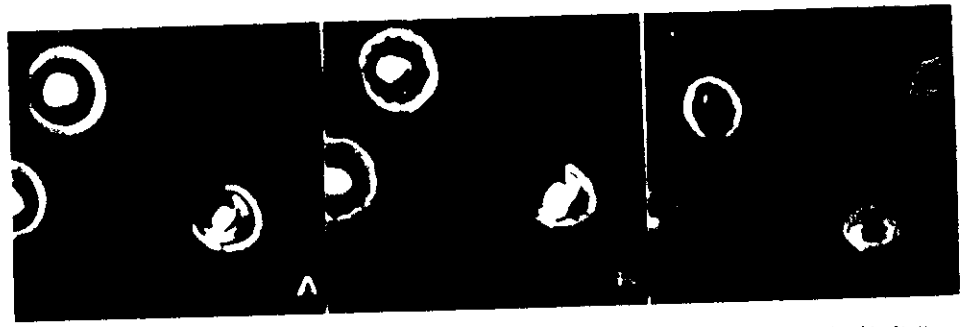


Fig. 2. - Transformation directe d'un stomatocyte (A) en un stomatocyte crênelé (B-C), observée au microscope à contraste de phases, par effet d'une micro-injection de salicylate de Na. Cinq secondes séparent la première image de la dernière.

21-001

RÉSULTATS

what physical variables are changed? (to modify shape)

CONCENTRATIONS FAIBLES

Les globules rouges lavés et transformés (fig. 1) par les faibles concentrations, indiquées plus haut. ~~de chlorpromazine et de prométhazine~~ sont capables de reprendre la forme discoeyte s'ils sont ensuite mis en suspension dans du plasma frais, ou s'ils sont lavés dans une solution de NaCl. Il faut noter que, dans le cas de la chlorpromazine et de la prométhazine, deux ou trois lavages peuvent être nécessaires, suggérant une fixation de ces substances au niveau de la membrane.

Le mélange de deux de ces substances, aux effets opposés, n'a aucune action sur la morphologie des globules rouges, permettant de croire à l'antagonisme de ces agents.

Les cellules, une fois induites en échinoctes, peuvent être changées en stomatoctes par l'action de la chlorpromazine. Au cours de la transformation, les cellules peuvent repasser par le stade discoeyte, mais de manière fugace. Lorsque la substance stomatoctaire est ajoutée tout d'abord, on obtient le phénomène inverse.

Parfois, pourtant, il semble que, dès que l'échinoctes a retrouvé sa concavité (Echinoctes 1), la cellule prend la forme en coupe sans reprendre totalement l'état discoeyte. On observe aussi, de temps en temps, une transformation directe d'un stomatoctes en un stomatoctes crénelé (cette cellule conserve la capacité de reprendre la forme discoeyte) (fig. 2). Ceci suggère que ces deux types d'agents, bien qu'antagonistes, n'agissent pas aux mêmes sites de la membrane et paraissent être des inhibiteurs non compétitifs. La séquence des transformations morphologiques induites par les faibles concentrations chimiques est représentée sur la figure 3, de 1 à 5.



Stomatocyte, III
D) Echinoctes Lc



gite crénelé (B-C),
-injection de salinière.

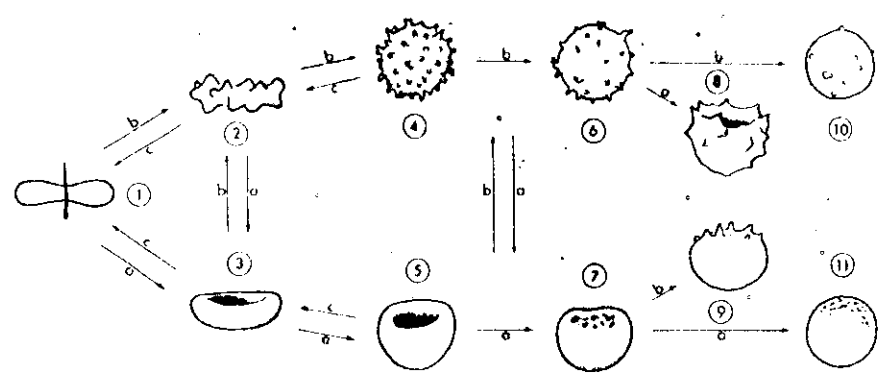


Fig. 3. — Le rapport et la convertibilité des formes discoeytaires, échinoctaires et stomatoctaires du globule rouge. La direction a indique un changement stomatoctaire; la direction b un changement échinoctaire; la direction c indique un effet permettant au globule rouge de reprendre la forme discoeytaire. Les cellules 10 et 11 évoluent vers l'hémolyse.

Symmetry

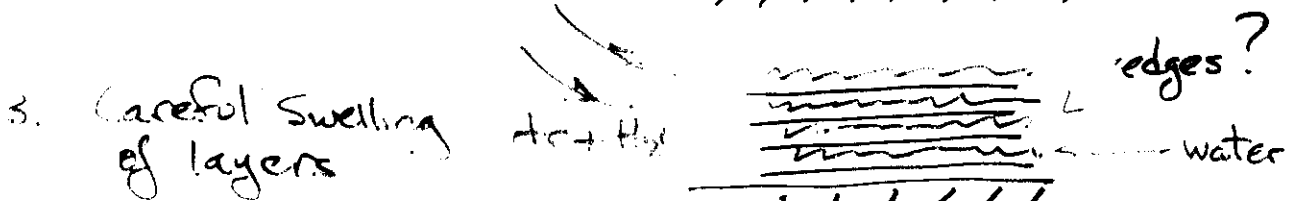
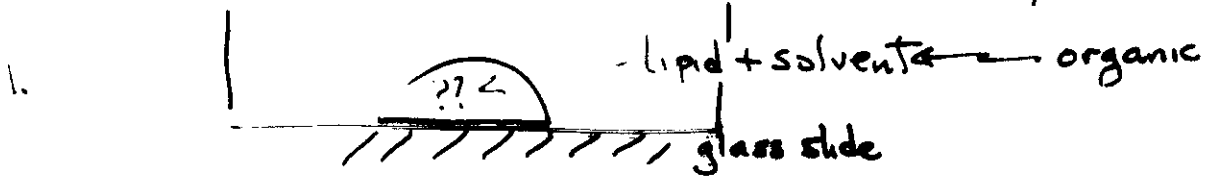
what is being manipulated in these transformations?

Do you see similar shapes and shape transitions for artificial vesicles?

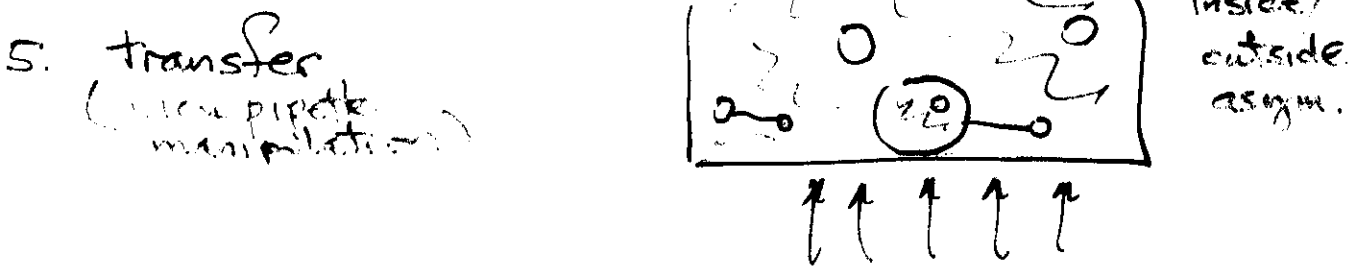
YES

Expt: Evans, (1980)

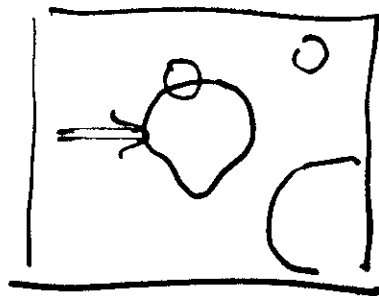
Produces S₀PC vesicles ~ 20 μm.



Closure mechanism is not known.



6. Phase Contrast Video microscopy through bottom of cell (gravity)

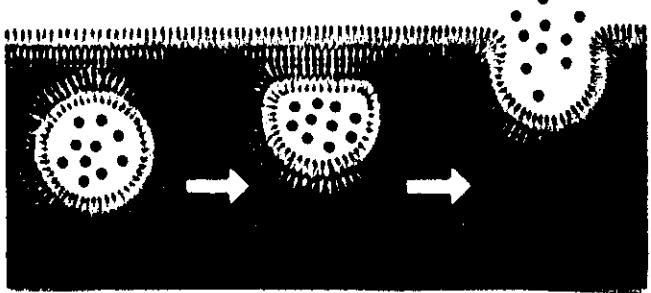


EXOCYTOSIS & ENDOCYTOSIS

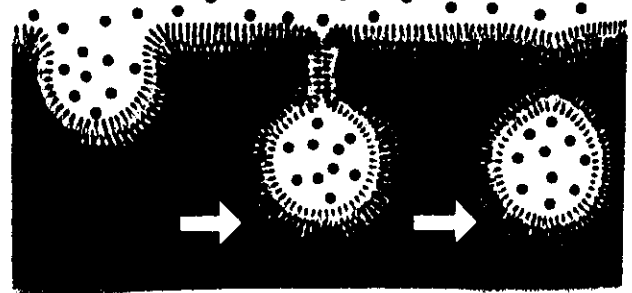
from Alberts et al., Molecular Biology of The Cell

biological importance of
shape transformations

EXOCYTOSIS



ENDOCYTOSIS



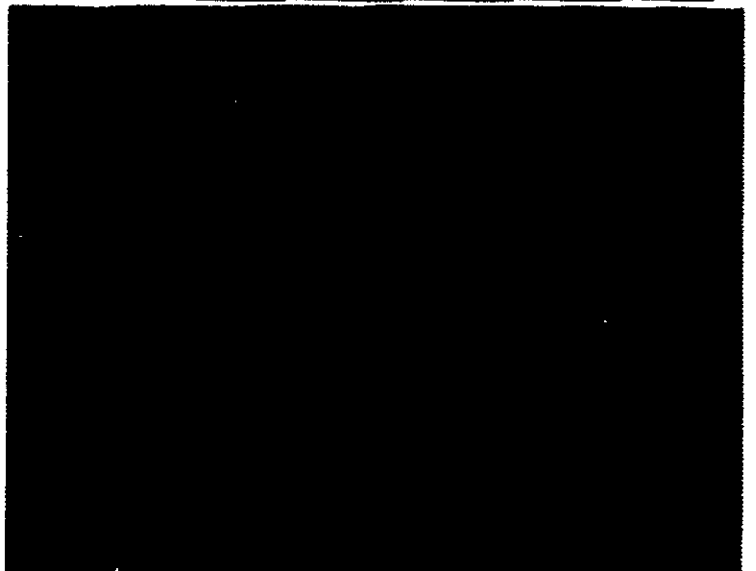
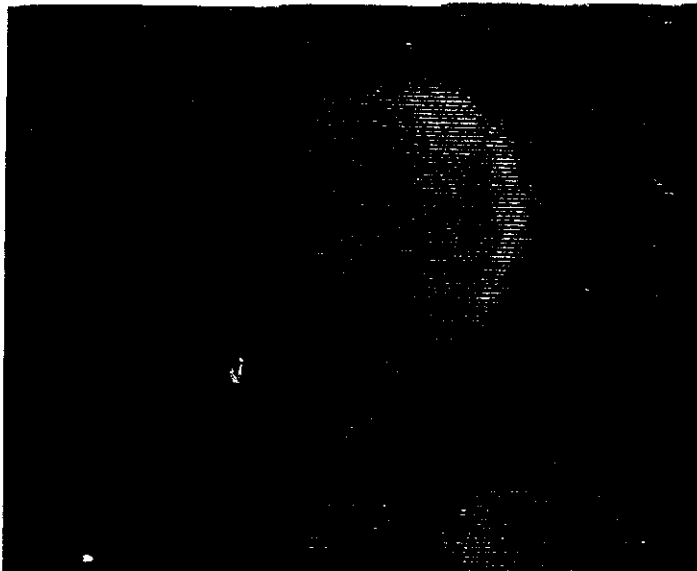
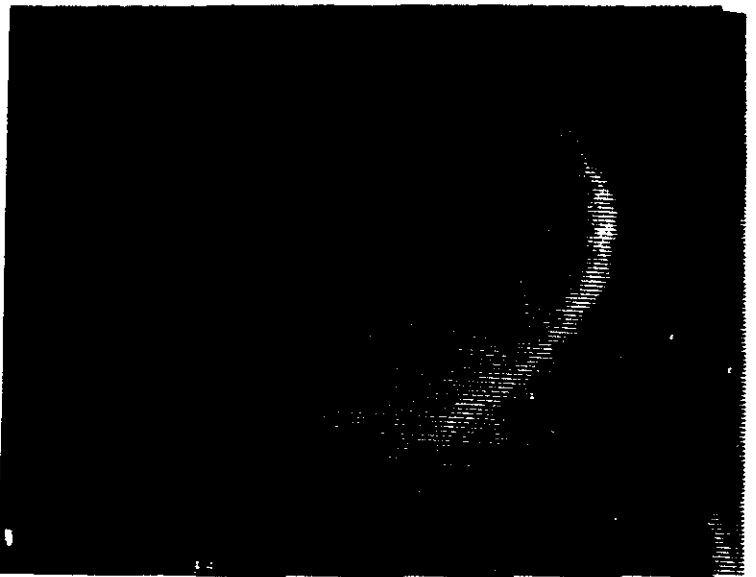
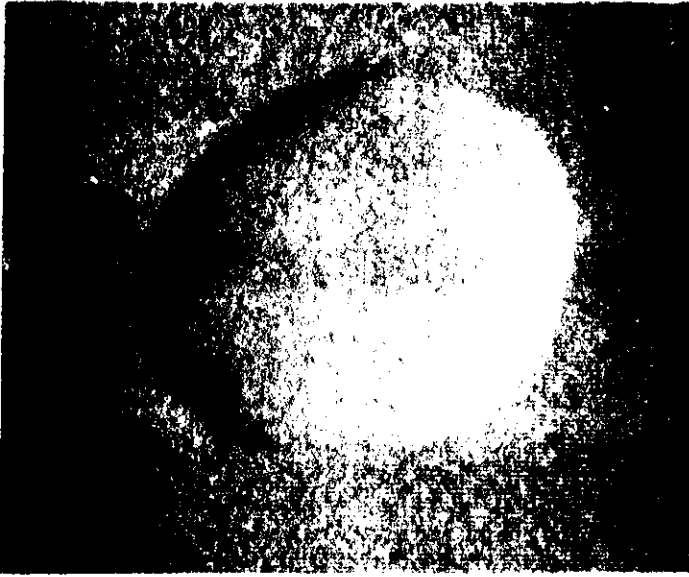
SUPC

T↑

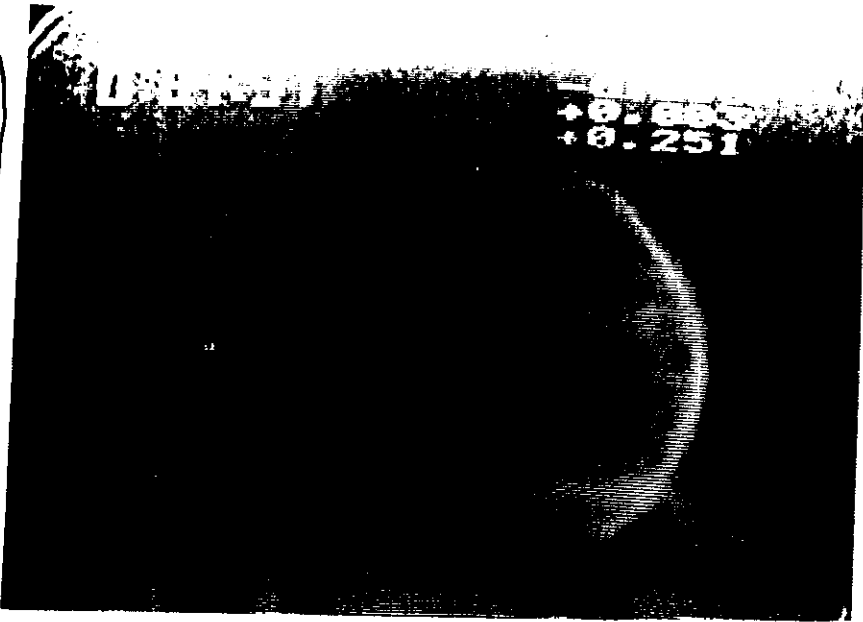
Lab of E. Evans.

Data: H-G D.

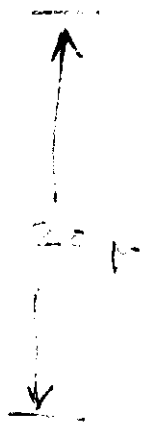
~ 5 μm



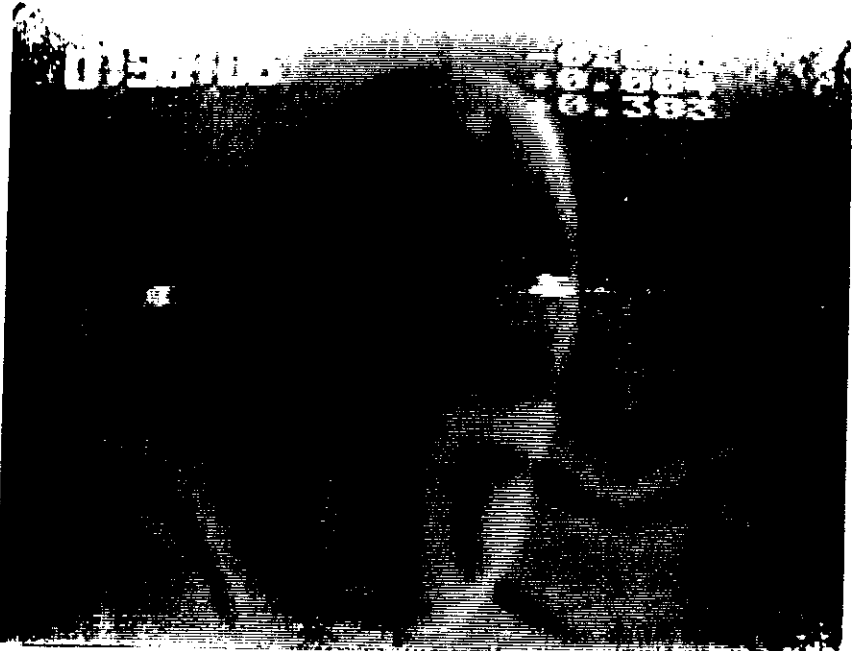
E. Evans
W. Rawlett
A. Young



12a

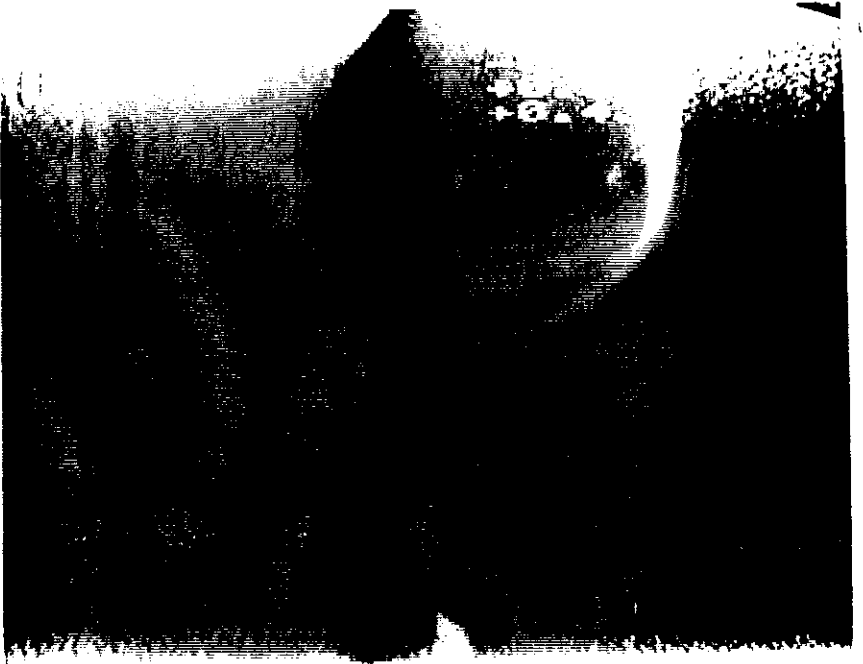


lecithin
(50 PC)
+
2-6%
neg. charged
lipid



differential
phase-
contrast
microscopy

Sequence.
volume ~ const.
area ↑



Morphology
change
at ~ 5%
excess area
(ΔA)

REVERSIBLE!

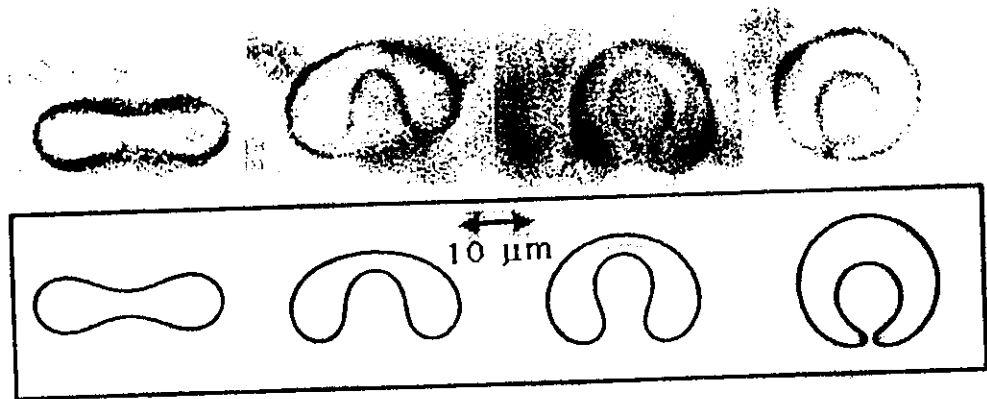
no
explanation

focus on "ball"
not tubule!

Berndl, Käs, Lipowsky, Sackmann, Seifert
DMPC (lecithin) artificial vesicles

SAVE 11
+13a

The discocyte - stomatocyte - transition. (4)



$T = (^{\circ}\text{C})$ 43.8 43.9 44.0 44.1

Note: Changing T is modifying
constraints: $A = A(T)$

$T \uparrow, A \uparrow$

model = bilayer-couple (ΔA -model)
 $\Delta H(T)$ need small differential
Thermal expansion



spermatocytes



testis?

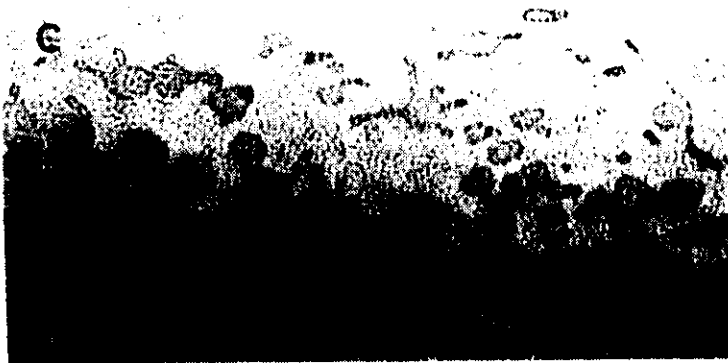
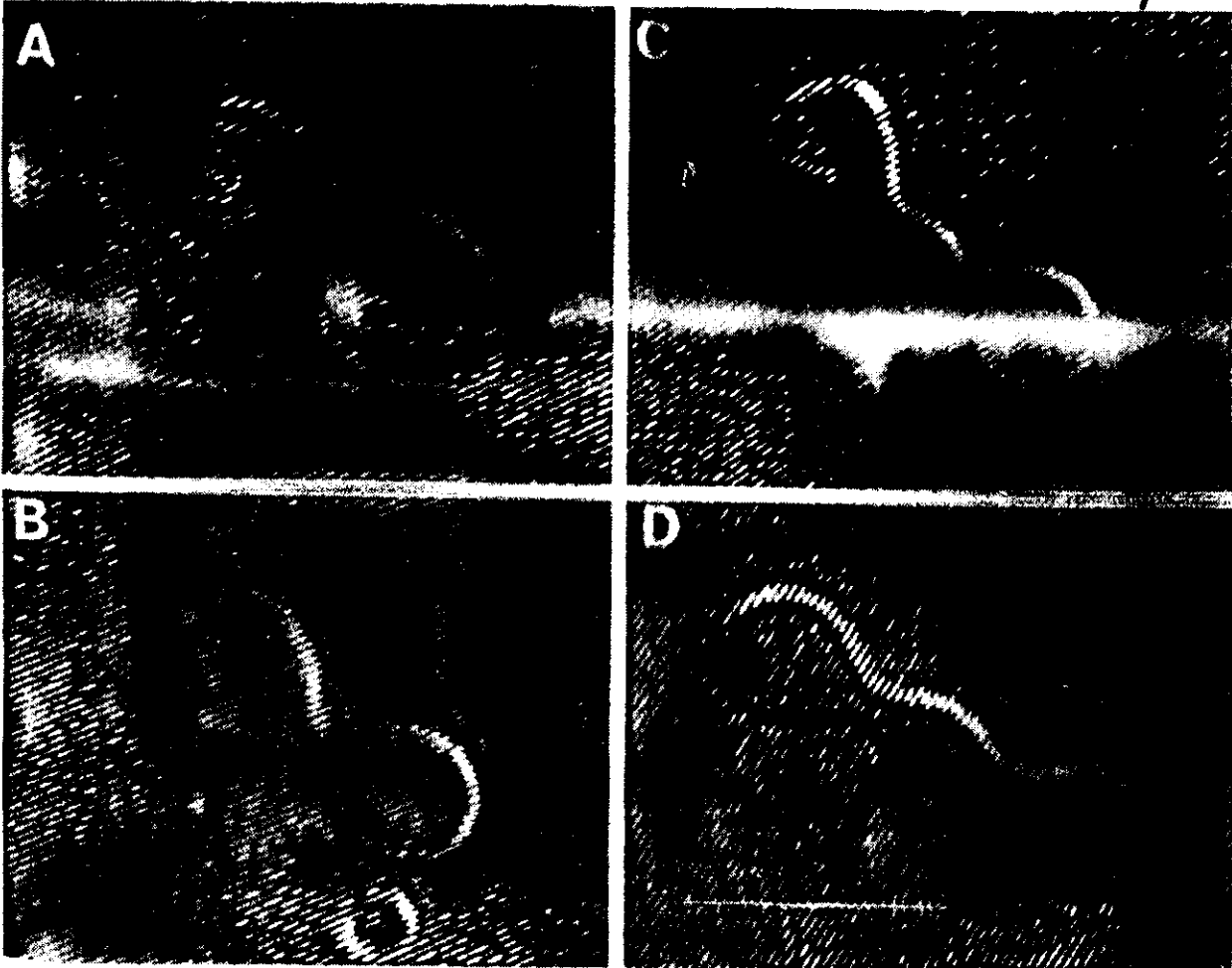
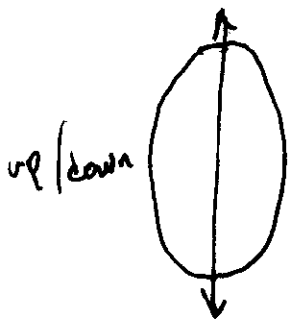


Fig 1



1.25 - 1.16 (1000)
Xfer to track ptt @ A \Rightarrow more EP (\rightarrow outside)
Sequence is 80 s.

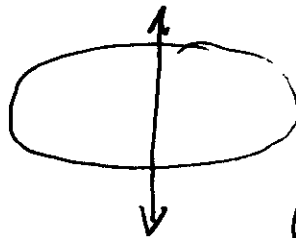
sphere



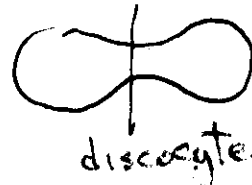
prolate.



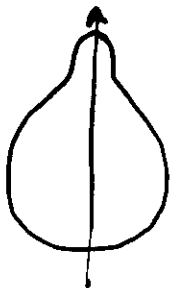
dumbbell



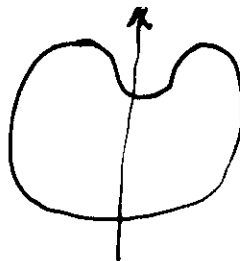
oblate.



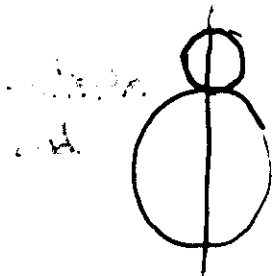
discocyte.



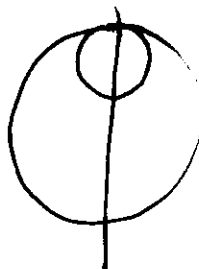
pear



stomatocyte.



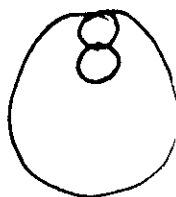
unstable (narrow neck)



unstable (narrow neck)



unstable (narrow neck)



Comment on narrow neck energetics

SHAPES (NAS)

3 inequival axes



"starfish"

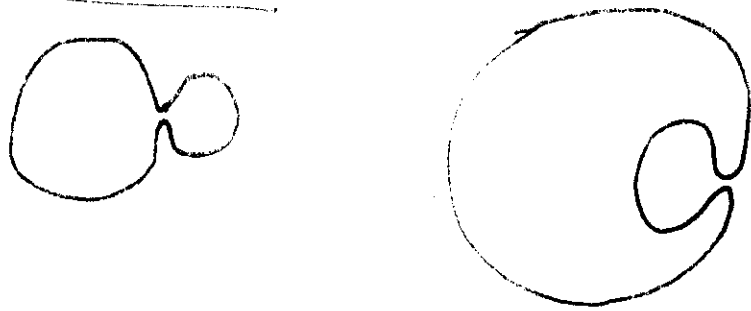
Seifert + Döbereiner

Also other topologies:
(Seifert) eg. tori

but not echinocytes

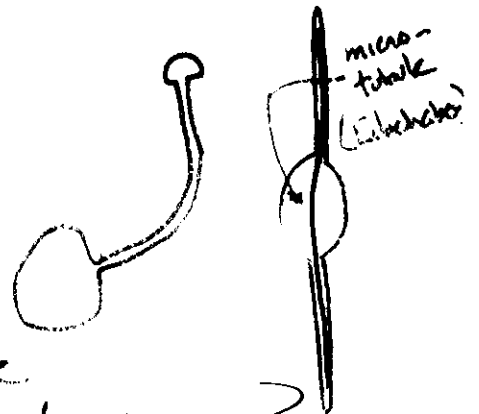
ALL these are seen to lab !!

Narrow necks:



- neck remains open
- easily drawn into microtube

prec Newton force balance



- how can these be low-energy structures?

$$\frac{K_b}{2} \left(\frac{1}{R_1} + \frac{1}{R_2} \right) \sim C_0$$

at neck $\frac{1}{R_1} \approx 0, \frac{1}{R_2} \ll 0$

at neck $\frac{1}{R_1} + \frac{1}{R_2} \sim \text{small}$ (needs $d=3$)

- locally. The neck region
 $\sim H=0$ "zero mean curvature."

- Contribution to bending energy (radius a)

$$\Delta E = \text{Const.} \times \underline{a} - \text{Const.} \underline{a^2} \underline{\kappa} + \dots$$

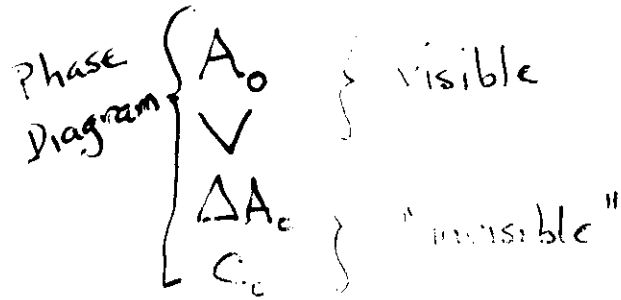
- "Kissing" Condition: $\frac{1}{R_1} + \frac{1}{R_2} = C_0$

Control Parameters:

Fixed V, A_0

$$H = \frac{\kappa_b}{2} \left[\int_S dS (c_1 + c_2 - g)^2 + \frac{\alpha \pi}{A_0 d^2} \left(d \int_S dS (c_1 + c_2) - \Delta A_0 \right)^2 \right]$$

κ_b irrelevant at T=0
 $\nu = \bar{\kappa} / \kappa_b$
 \perp } assume $\nu = 0$



Overall length scale: Dilation "Reduced" variables Biology controls shape via biochemical adjustment of $C_0, V, \Delta A_0$

Let $A_0 = 4\pi R_A^2$

$C_0 \rightarrow R_A C_0$

$V \rightarrow \nu \equiv \frac{V}{\frac{4\pi}{3} R_A^3}$

$\Delta A_0 \rightarrow \Delta a_0 \equiv \frac{\Delta A_0}{8\pi d R_A}$

$\Delta a_0 < 0 \quad \nu_{in} > \nu_{out} \quad \odot$

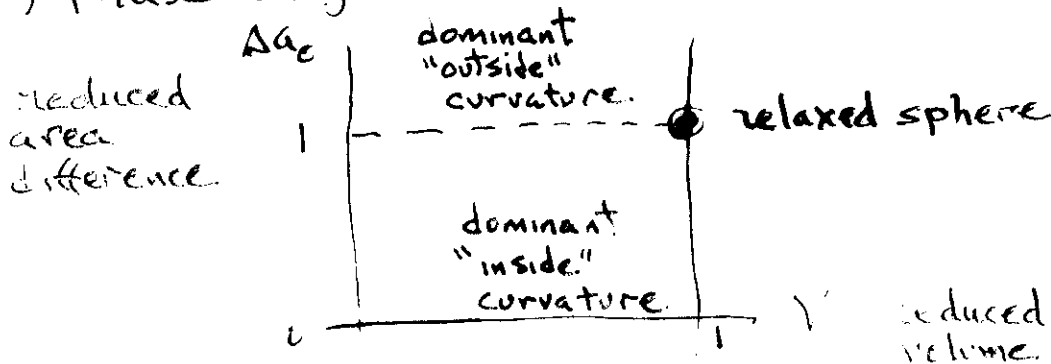
$\Delta a_0 > 0 \quad \nu_{in} < \nu_{out} \quad \ominus$

Under variation:

$$c_i \rightarrow C_0 = c_0 - \frac{\alpha \pi}{A_0 d} (A[S] - \Delta A_0)$$

effectively combines C_0 and ΔA_0 (self-consistency)

Shape) Phase Diagram:



Comment on Control Parameters

One overall length scales out of energy
 ("isometric" integrals)

Let: $A \equiv 4\pi R_A^2$

$C_0 \rightarrow c_0 \equiv R_A C_0$

"reduced volume"

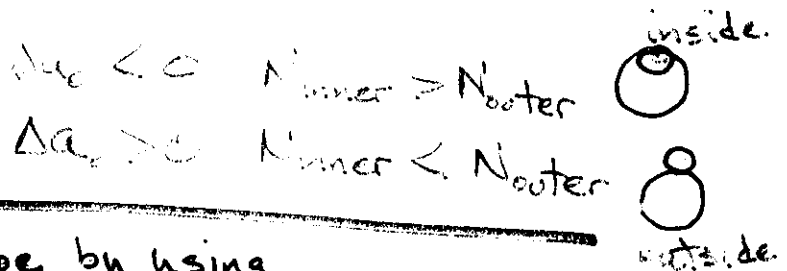
$V \rightarrow v \equiv \frac{V'}{\frac{4}{3}\pi R_A^3}$

$v = 1$ sphere (ONLY)
 $0 \leq v \leq 1$

"reduced area difference"

$\Delta A_0 \rightarrow \Delta a_0 \equiv \frac{\Delta A_0}{8\pi D R_A}$

$\Delta a_0 = 1$ for relaxed spherical vesicle.



Biology can "control" shape by using biochemical mechanisms to adjust
 The control parameters $\alpha, c_0, v, \Delta a_0$

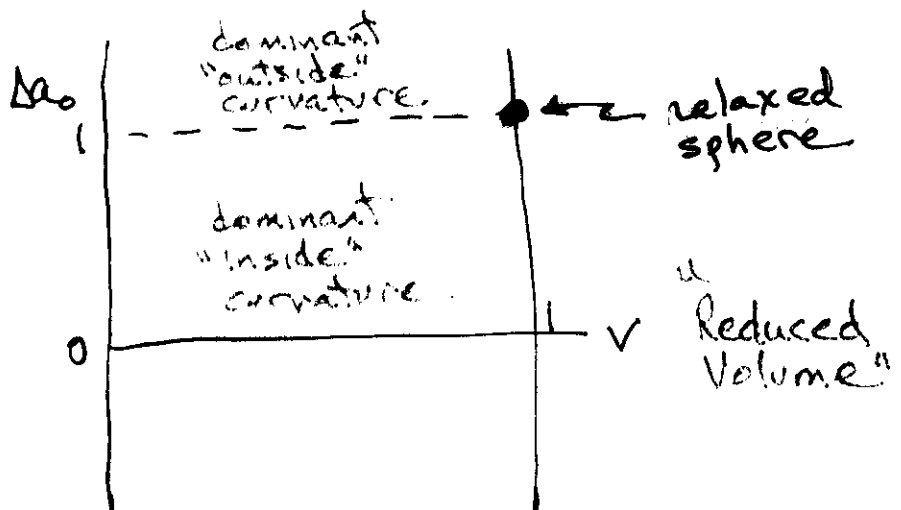
But does it?

(Shape) Phase Diagram:

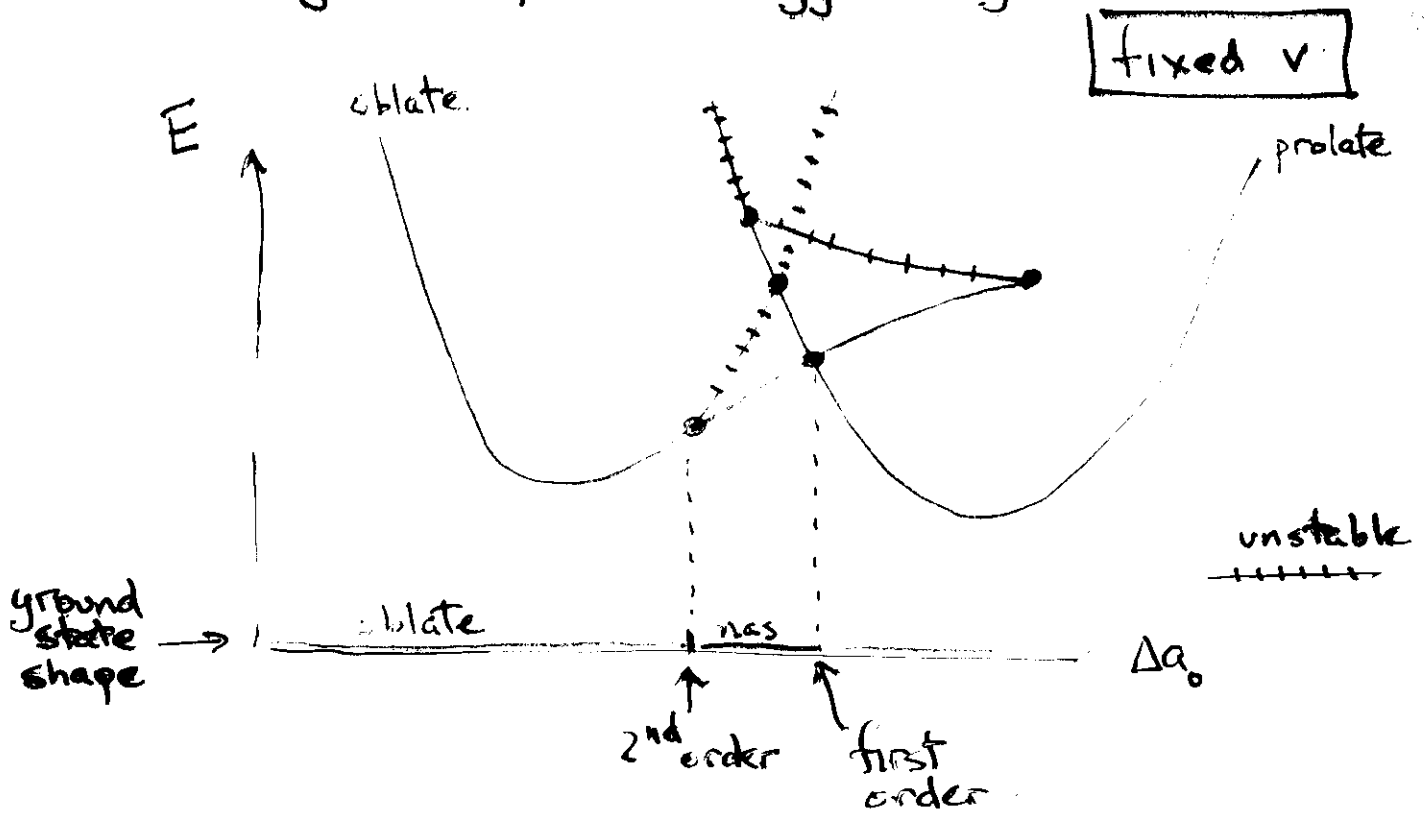
for Two shapes

(c_0, α fixed)

Reduced Area Difference

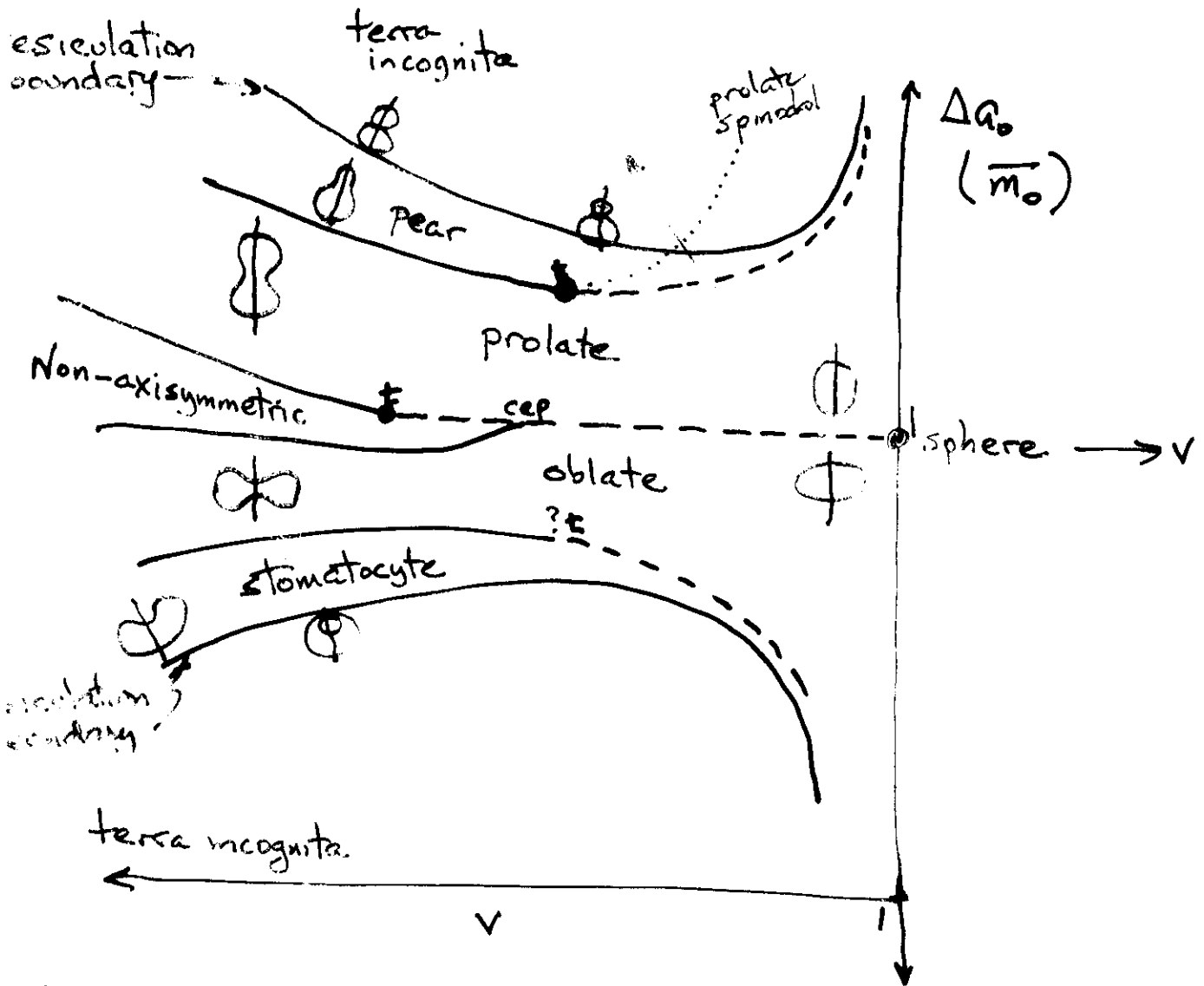


Stationary - Shape - Energy Diagrams



Phase Diagram at $\frac{\bar{K}}{K_b} \sim 1$

incl. data of V. Heinrich + Wang



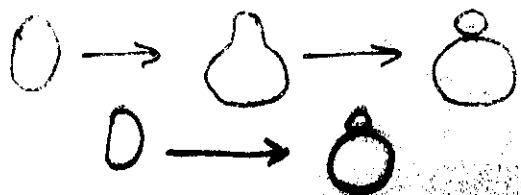
Key — continuous (2nd order)
 - - - discontinuous (1st order)
 t tricritical

α -dependence of phase diagram

trajectories

metastability

prolate \rightarrow pear \rightarrow vesiculated transition



$$\Delta u_c = \frac{\bar{m}_0}{4\pi}$$

$$\alpha = 1.4 \quad (\text{DMPC})$$

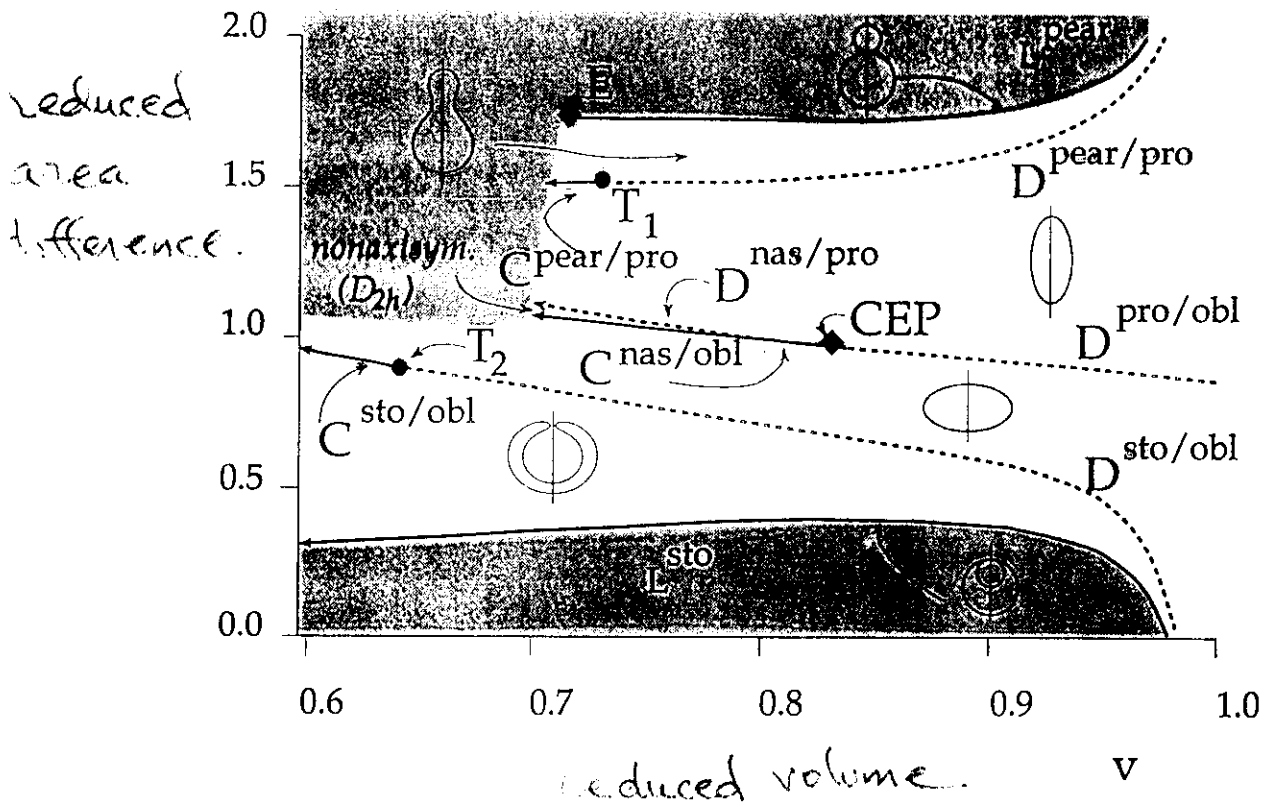


Fig. 2 (Nicolai)

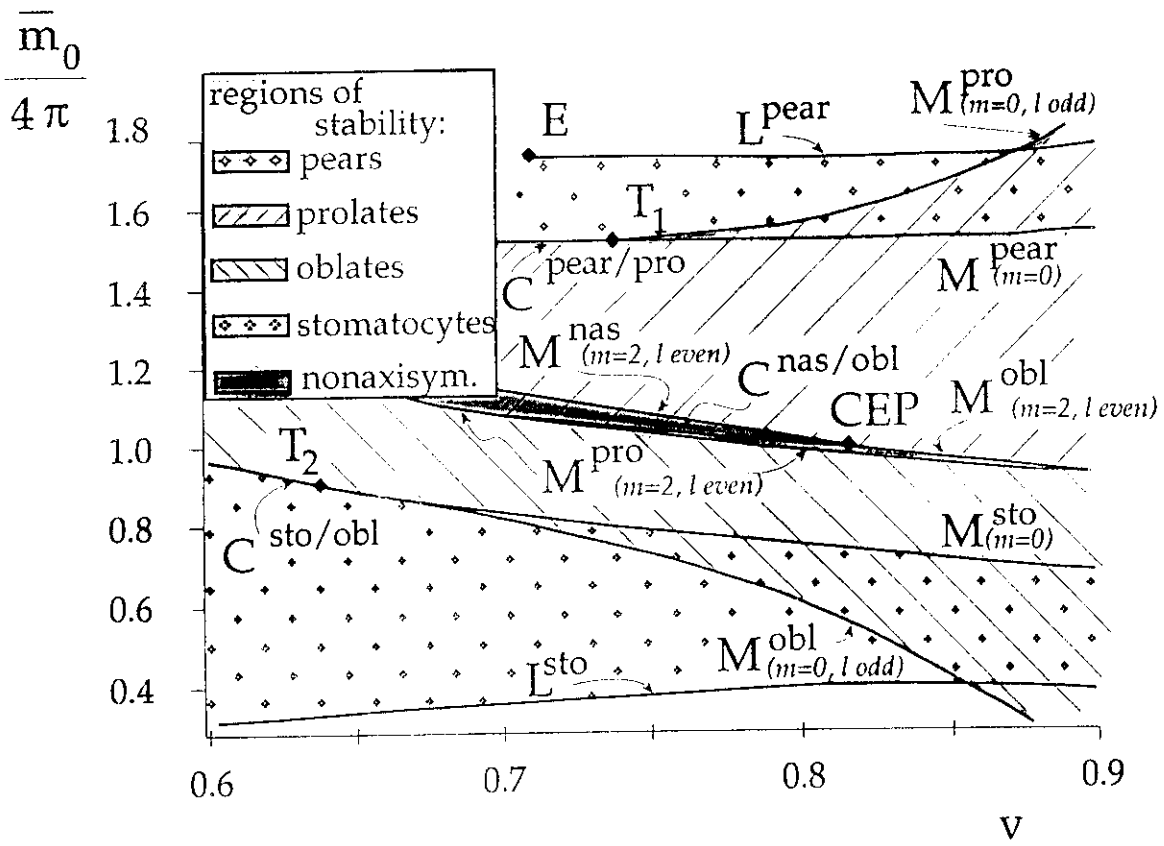
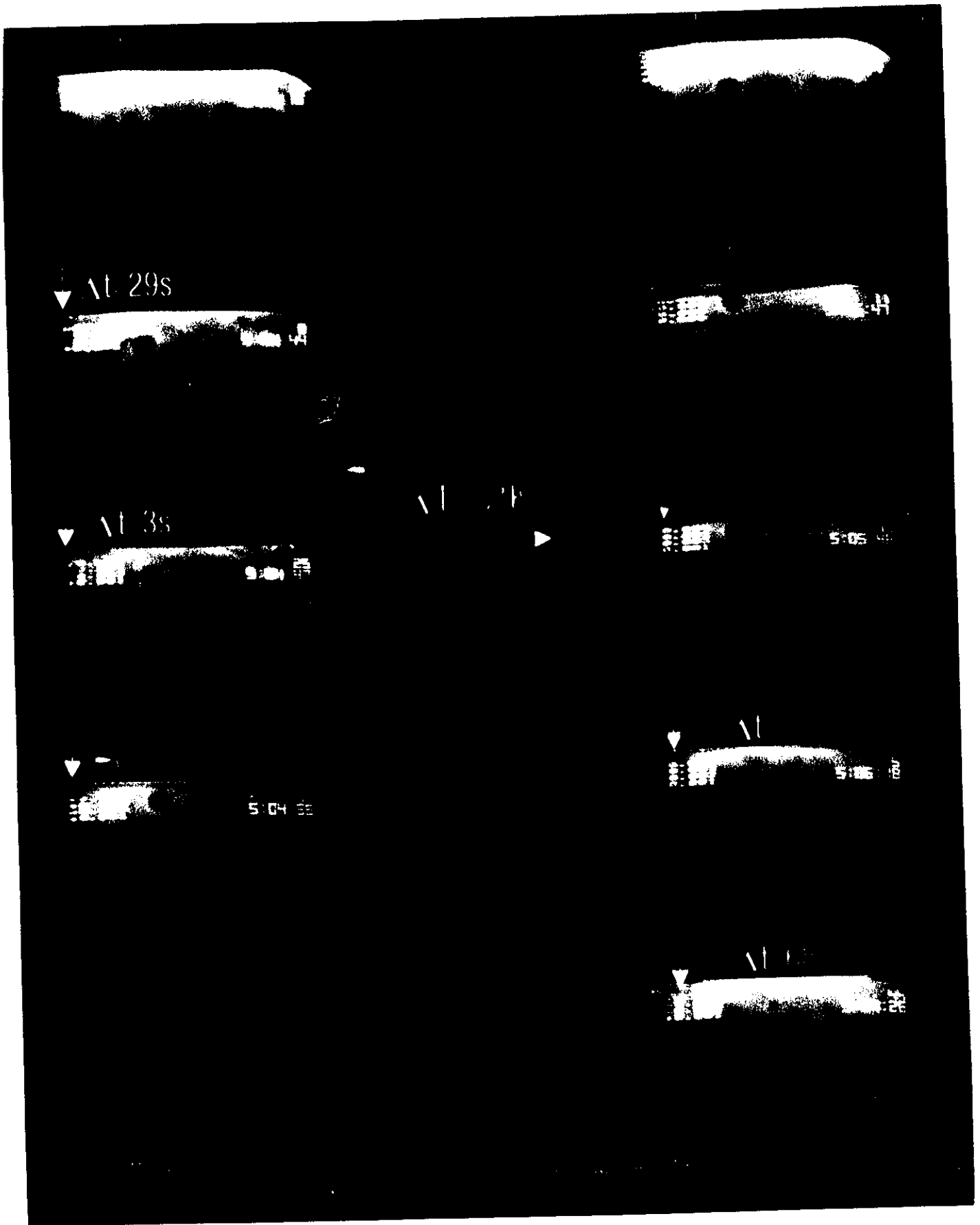


Fig. 3 (Nikolic et al)



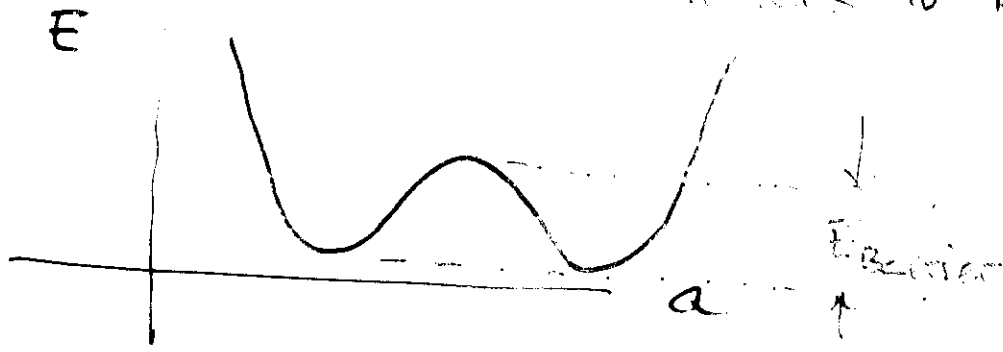
Shape Fluctuations, Metastability, & "Spinodal" Behavior

thermally driven shape fluctuations are observed & can be important in lab.

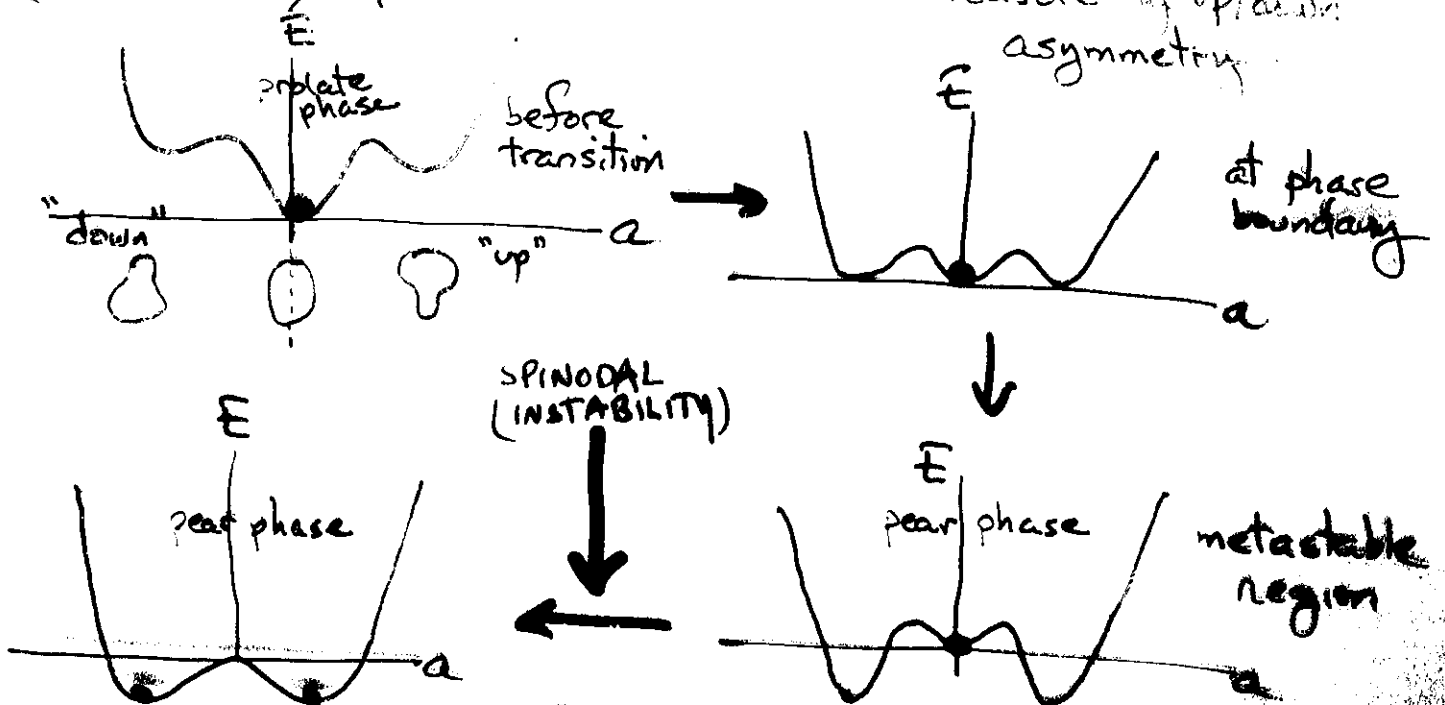
slide

for any $T > 0$ "phase" boundaries are (in principle) fuzzy.

but no position until barriers $\sim k_B T$



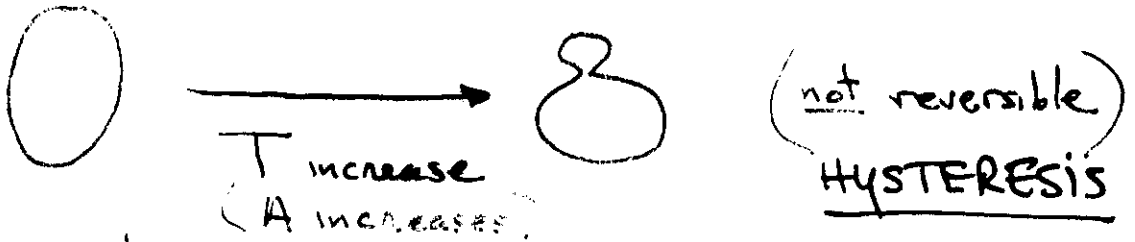
(First-order) Spinodal behavior: μ = measure of up/down asymmetry



(in lab) \Rightarrow large fluctuations + slow timescales near "spinodal"

Observation of "The budding instability"

Evans
Sackmann
Käs
Döbereiner

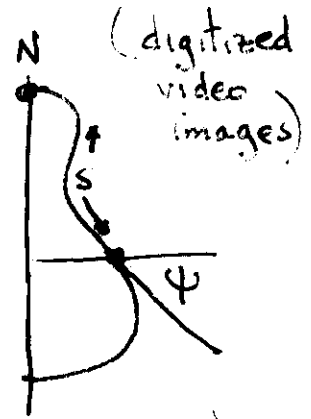


- large shape fluctuations just before transition
- soft mode "quasi-critical fluctuations"
- slow dynamics "quasi-critical slowing down" *

spindal instability

mode analysis of shape fluctuations:

$$\psi(s) = \underbrace{\pi \frac{s}{s^*}}_{\text{circle}} + \sum_{n=1}^{\infty} a_n \sin(n\pi \frac{s}{s^*})$$

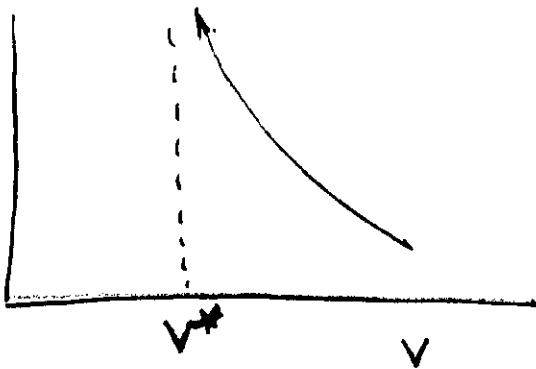


$\langle a_n \rangle$

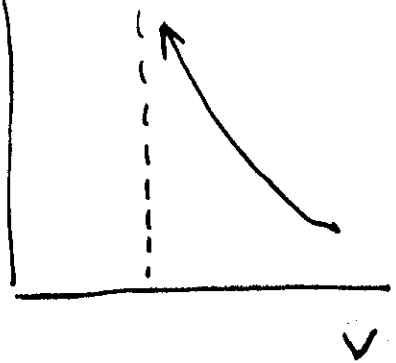
$$\langle (a_n(t) - \langle a_n \rangle)(a_n(0) - \langle a_n \rangle) \rangle \equiv C_n(t)$$

dominant exponent decay τ_n

$\langle a_3^2 \rangle$



τ_3

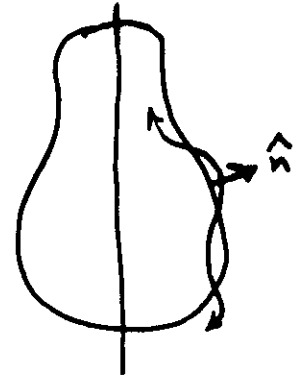


Fluctuations about $T=0$ Shapes (axisymmetric)

subject to "hard" constraints

$$[s] \equiv \vec{R}(s_1, s_2)$$

$$= R_0(s_1, s_2) + \epsilon(s_1, s_2) \hat{n}(s_1, s_2)$$



$$\epsilon(s_1, s_2) = \sum_{l,m} a_{lm} Y_{lm}(\pi \frac{s_1}{2\pi}, \varphi)$$

- Constraints $V[s] = V[s_0] \equiv V_0$
 $A[s] = A[s_0] \equiv A_0$

- Removal of Euclidean modes

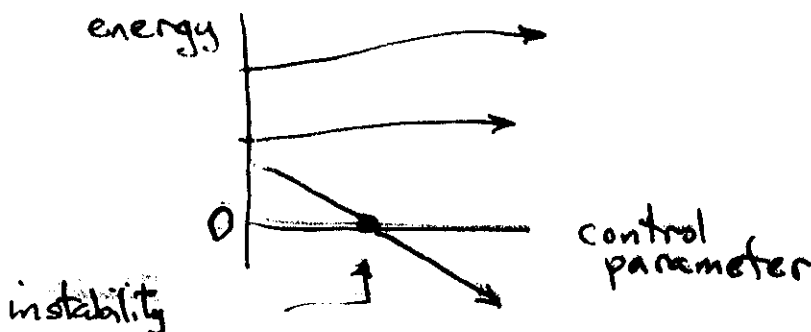
Projection of Constraints

\Rightarrow problem of physical energy eigenmodes of fluctuation.

Sectors: $|m|$ (axisymmetry)
 l -even/odd (up/down)

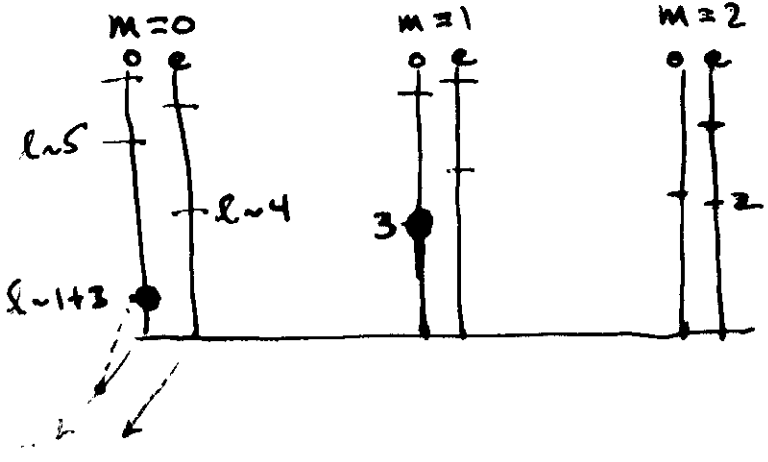
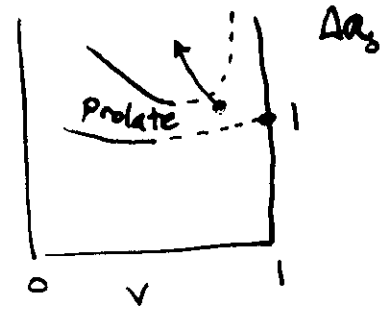
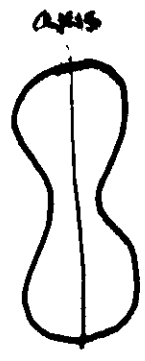
Fluctuation modes ω_n, ρ_n

Soft modes near instability:



Example:

Fluctuations of
up/down asymmetric
prolate shape



"pear" fluctuation
(SFT at budding
spinodal)



"banana" fluctuation

Does biology "use" these shape mechanics?

Every case is different.

A. Red blood-cell shapes:

Yes (??). But, structure is complicated.
and mechanisms of control of A, V, C_0
incompletely understood.

B. Budding processes: PM
Golgi

- Often controlled by proteins (clathrins)
(not always ??)
- May have played more role
early in evolution (??)
- Energy scale is right!

C. Other budding mechanisms:

Real membranes have many lipids (10^3 !)

Domain-induced budding (Lipowsky)

